THE JOURNAL OF PHYSICAL CHEMISTRY A

Article

pubs.acs.org/JPCA

Electronic Relaxation after Resonant Laser Excitation of Cr in Superfluid Helium Nanodroplets

Andreas Kautsch, Markus Koch,* and Wolfgang E. Ernst*

Institute of Experimental Physics, Graz University of Technology, Petersgasse 16, A-8010 Graz, Austria, EU

ABSTRACT: Chromium (Cr) atoms embedded into helium nanodroplets (He_N) are ejected from the droplets upon photoexcitation. During ejection they undergo electronic relaxation resulting in bare Cr atoms in various excited states. In a study of the relaxation process we present absorption spectra observed via laser induced fluorescence and beam depletion as well as dispersed fluorescence spectra and time-resolved fluorescence measurements. Broad and shifted absorption structures were found for the strong $z^7P^\circ \leftarrow a^7S_3$ and $y^7P^\circ \leftarrow a^7S_3$ excitations from the ground state. Emission lines are, in contrast, very narrow, which indicates that fluorescence is obtained from bare excited Cr atoms after ejection. Upon excitation into the $y^7P^\circ_{2,3,4}$ states we observed fluorescence from $y^7P^\circ_2$, $z^5P^\circ_{1,2,3}$, and $z^7P^\circ_{2,3,4}$, indicating that these states are populated by electronic relaxation during the ejection processes. Relative population ratios are obtained from the intensities of individual spectral lines. Excitation into the $z^7P^\circ_{2,3,4}$ states resulted in fluorescence only from $z^7P^\circ_2$. Estimates of the time duration of the ejection process are obtained from time-resolved measurements.

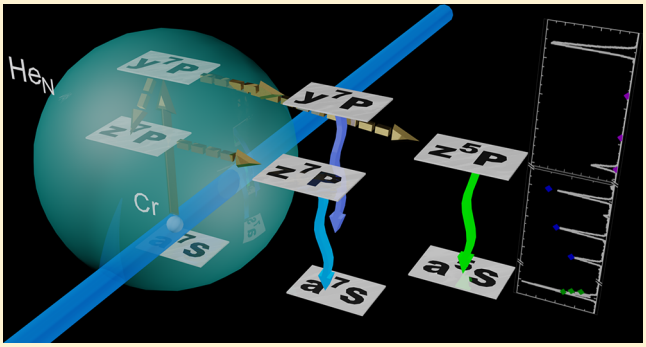

INTRODUCTION

Chromium (Cr) is of astrophysical interest because of its presence in astronomical objects[1,2] and in the solar spectrum.[3] Cr atoms and molecules have been isolated in rare gas matrixes for spectroscopic studies.[4] With regard to the free atoms, these studies find blue shifts and line broadenings of absorption spectra in the range of a few cm^{-1} to several 1000 cm^{-1}, depending on the change in electron configuration caused by the excitation. Matrix perturbations on Cr emission lines are found to be relatively small (<100 cm^{-1}). Upon excitation from the a^7S_3 ground state (electron configuration [Ar] $3d^54s^1$) via the two strong resonant transitions to $z^7P^\circ_{2,3,4}$ ($3d^54p$) and $y^7P^\circ_{2,3,4}$ ($3d^44s4p$), the Cr atoms were found to undergo complete electronic relaxation (also to states with different spin multiplicities) and fluorescence of matrix isolated Cr atoms was observed exclusively from other states than those originally excited.

In terms of matrix isolation, superfluid helium nanodroplets (He_N) combine many advantageous properties. Because of their low temperature of 0.37 K, their confinement character and very versatile doping possibilities, they have been popular for spectroscopic investigations of cold atoms, molecules and clusters.[5] We have recently succeeded in doping He_N with Cr atoms.[6] In a first spectroscopic study we identified the photoinduced ejection of bare Cr in the $z^5P^\circ_J$ (J = 1−3 being the total angular momentum quantum number) states.[7] The population ratios of the different J components could be obtained from an evaluation of the line strengths of transitions to autoionizing states.

In this work we present absorption spectra for the $z^7P^\circ_{2,3,4} \leftarrow a^7S_3$ and $y^7P^\circ_{2,3,4} \leftarrow a^7S_3$ excitations, which are obtained from laser induced fluorescence and beam depletion. To further investigate the ejection and relaxation process, dispersed fluorescence spectra are presented. Finally, estimates for the duration of the ejection and relaxation process are obtained from time-resolved laser induced fluorescence measurements.

EXPERIMENTAL SECTION

The experimental setup is based on a helium nanodroplet isolation spectroscopy apparatus described in detail elsewhere.[8] In brief, the helium nanodroplets are formed by a supersonic expansion of precooled (19 K) high purity He (99.9999%) from 50 bar into vacuum through a 5 μm nozzle (maximum of droplet size distribution: $\hat{N} \approx 1800$). The droplets pass through a 300 μm skimmer into a separately pumped pickup chamber in which chromium metal is evaporated by a home-built high temperature electron bombardment source.[6] The Cr beam is crossed with the He_N beam at right angles along 10 mm of the He_N flight path. With this crossed beam geometry it can be ensured that no free atoms reach the detectors. The heating power of the Cr source is optimized for single atom pick up.

Special Issue: Oka Festschrift: Celebrating 45 Years of Astrochemistry

Received: December 14, 2012
Revised: February 14, 2013
Published: February 14, 2013

   dx.doi.org/10.1021/jp312336m | J. Phys. Chem. A 2013, 117, 9621−9625

In the main chamber laser induced fluorescence (LIF) and laser induced detachment of Cr from He_N (i.e., beam depletion, BD) can be detected. For LIF measurements the beam of doped He_N is crossed by a laser beam at right angles. Baffle stacks are used to reduce stray light and ambient light. LIF light is collected by a combination of an aspheric lens (o.d. 40 mm, f = 29 mm) and a concave mirror (o.d. 33 mm, f = 10 mm). Collected light is guided through an aperture for spatial filtering and detected by a photomultiplier tube (PMT) (EMI 9558QB, EMI 9863/350QB). For time-resolved fluorescence measurements band-pass or low-pass filters can be inserted in front of the PMT to monitor fluorescence light of individual transitions. Electronic pulses from the PMT are amplified (Ortec VT120A) and counted (Stanford Research Systems SR 400). When spectra are recorded with pulsed lasers (see below), a 60 ns detection gate is triggered by a fast photodiode. For time-resolved LIF measurements a 5 ns counting gate is scanned in 1 ns steps. For dispersed fluorescence measurements the emitted light is passed through a monochromator (McPherson EU-700) with an attached CCD camera cooled to −100 °C (LOT-Andor iDUS DU401A BR-DD). To compare intensities of emission lines from different excited states, we calibrated the detection system with a calibrated tungsten ribbon lamp.

To detect BD, a quadrupole mass spectrometer (QMS, Balzers QMG 422) is located at the end of the main chamber. The QMS rod system is oriented at right angles to the droplet beam so that the latter can be counterpropagated by a laser beam. Doped He_N are ionized by electron bombardment and ions are extracted toward the rod system, mass filtered, and finally detected by a secondary electron multiplier. The mass filter was set to 52 amu, the mass of the most abundant Cr isotope. Note that Doppler shifts due to the counter propagating arrangement can be neglected with respect to the broadening of excitation lines inside He_N. Electronic pulses from the QMS are amplified (home-built amplifier), discriminated and counted (Stanford Research Systems SR 400). Signal fluctuations due to source instabilities are reduced by applying a differential counting scheme (laser on QMS signal minus laser off QMS signal).

For BD, undispersed LIF, and time-resolved fluorescence measurements, nanosecond laser pulses were used. The laser pulses were obtained from an excimer (XeCl, Radiant Dyes RD-EXC-200) pumped dye laser (Lambda Physik FL3002, dyes RDC 360 and Stilbene 3) with 20 ns pulse duration and 100 Hz repetition rate. For dispersed fluorescence measurements two different continuous wave (cw) laser systems were used. A frequency doubled Ti:sapphire laser (Coherent Verdi V18 pump laser, Coherent 899 in single mode and Toptica TA-SHG 110, maximum power output 150 mW) at 23600−23900 cm^{-1} was used for excitation into the $z^7P°$ states, and a Kr ion laser (Coherent Innova Sabre, maximum power output 400 mW) at 28048.64 cm^{-1} was used for excitation into the $y^7P°$ states.

RESULTS AND DISCUSSION

To discuss our results, we start with the characteristics of the excitation spectra followed by the observations of the fluorescence from the $z^7P°$ ($3d^54p$) and $y^7P°$ ($3d^44s4p$) states. For illustration, Figure 1 displays a level diagram of Cr indicating excitation (upward pointing arrows), relaxation (dotted arrows), and fluorescence (downward pointing arrows) paths observed. Laser excitation around the strong transitions $z^7P°_{2,3,4} \leftarrow a^7S_3$ (23305.01, 23386.35, and 23498.84 cm^{-1}) and

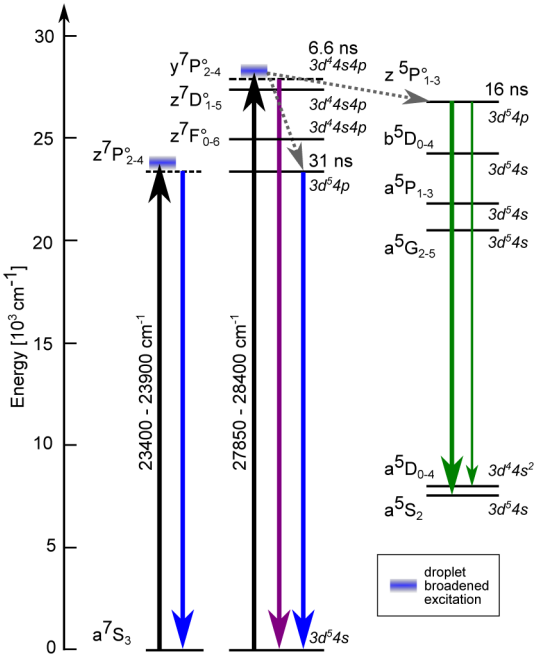

Figure 1. Level diagram of Cr and observed absorption and emission paths. Shaded rectangles indicate the excitation broadening due to the He_N and dashed lines stand for states where only emission from the lowest J substate could be observed. Nonradiative relaxation processes are marked as dotted arrows. Approximate lifetimes are shown next to some excited states of interest.[9]

$y^7P°_{2,3,4} \leftarrow a^7S_3$ (27728.87, 27820.23, and 27935.26 cm^{-1}) leads to BD spectra as shown in Figure 2. For the $y^7P° \leftarrow a^7S_3$ transition the LIF excitation spectrum is also shown for

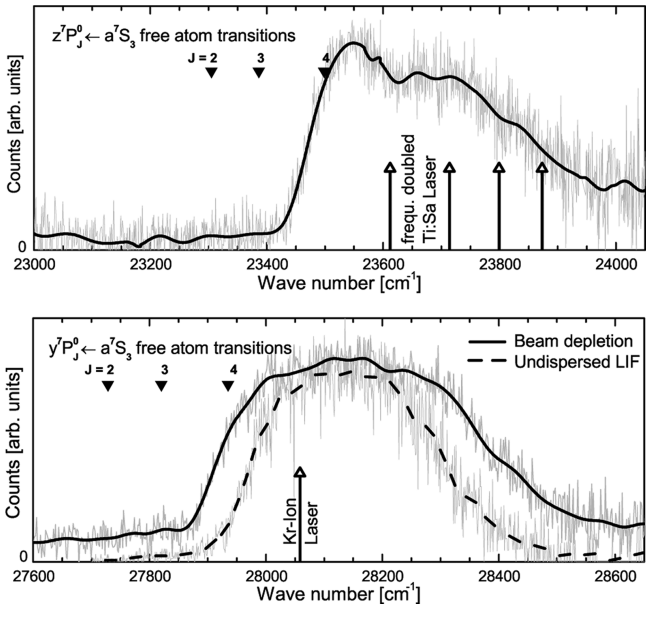

Figure 2. Beam depletion spectra of Cr atoms doped to He_N in the $z^7P° \leftarrow a^7S_3$ and $y^7P° \leftarrow a^7S_3$ transition region. For comparison, the lower graph shows the LIF detected excitation spectrum (dashed line). The measured signal (gray) is low pass FFT smoothed (black) and triangles indicate the free atom excitation transitions taken from ref 12. Excitation wave numbers for dispersed LIF measurements using the Kr ion and frequency doubled Ti:sapphire lasers are indicated (cf. Figures 3 and 4).

dx.doi.org/10.1021/jp312336m | J. Phys. Chem. A 2013, 117, 9621−9625

comparison in the lower graph. Further broadening occurred in our experiments at higher laser fluence of the pulsed laser indicating saturation effects, e.g., in BD (115 μJ) compared to LIF (<10 μJ). The broad excitation band agrees with our former photoionization (PI) experiment.[7] Compared to free atom transitions, a blue shift of approximately 300 cm^{-1} is measured. Similar, but much stronger, shifts were observed for Cr dopants in matrixes (Ar, Kr) with up to 1400 cm^{-1}.[4] Furthermore, the peaks are broadened so that they give rise to one structure expanding over ~450 cm^{-1}. In matrix experiments, it was also not possible to resolve the *J*-splitting of lines due to the strong broadening.[4] For Ag in He_N, similarly shaped excitation structures were found.[10] The strongly shifted and broadened excitation can be taken as indication for the solvation of Cr inside the droplet. In a liquid or solid matrix it is a consequence of the orbital's size change from the ground to the excited state. Upon excitation into a larger orbital, strong Pauli repulsion of the surrounding helium causes the shift and the broadening.[5,10,11]

The dispersed fluorescence after excitation into various parts of the $z^7P°$ and the energetically lower side of the $y^7P°$ excitation band are shown in Figures 3 and 4, respectively.

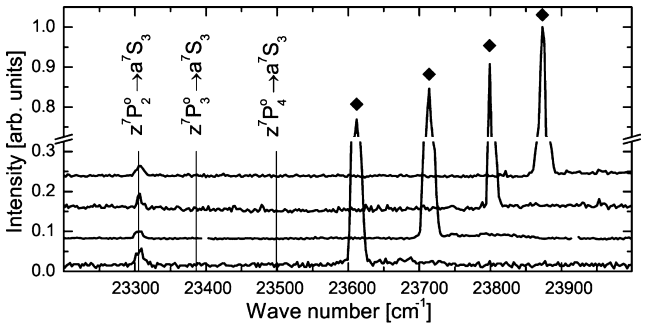

Figure 3. Dispersed fluorescence of Cr atoms upon excitation through the $z^7P° \leftarrow a^7S_3$ transition inside He_N at differing photon energies (plots mutually shifted in vertical direction, laser marked with squares). Vertical lines indicate the free atom transitions $z^7P^o_{2,3,4} \rightarrow a^7S_3$.[12]

Scattered laser light serves as a reference marker. Clearly, all major emission[12] takes place at the free atom transition wavelengths within the relative uncertainty of the monochromator measurement (measured line widths are shown in Table 1). If the emitting atoms were still attached to the droplets, line shifts and broadening beyond the resolution of the monochromator (4−8 cm^{-1}) should be observed. We conclude that all measured emission spectra result from free Cr atoms that had left the droplets.

With the laser excitation into $z^7P°$ ($3d^54p$) or $y^7P°$ ($3d^44s4p$) levels the related radiative emission to the ground state represents the dominant portion of the spectra. Matrix isolated Cr atoms show nonradiative energy relaxation mechanisms leading to no detectable fluorescence signals from these states.[4] On the other hand, from the $z^7P^o_{2,3,4} \rightarrow a^7S_3$ and $y^7P^o_{2,3,4} \rightarrow a^7S_3$ spin−orbit components only the energetically lowest transition is present ($z^7P^o_2 \rightarrow a^7S_3$, $y^7P^o_2 \rightarrow a^7S_3$). This phenomenon has no dependence on the excitation wavelength within the excitation region (Figures 2 and 3). So, a full relaxation within the *J* splitting of these excited states can be assumed and clearly bears the signature of the He_N influence. In our experiments, the fluorescence emission after the $z^7P°$ excitation turned out to be very weak, which may be attributed to quenching processes. Contrary, after excitation into $y^7P°$ the direct $y^7P^o_2 \rightarrow a^7S_3$ emission exceeds all other transitions in intensity.

After excitation into the higher energetic $y^7P°$ ($3d^44s4p$) band, also the energetically lower $z^7P^o_{2,3,4}$ ($3d^54p$) and $z^5P^o_{1,2,3}$ ($3d^54p$) states become populated and free atom allowed transitions from these levels contribute to the observed spectrum. In this case, emission from all substates is clearly present. Even weak transitions of $z^5P^o_{2,3} \rightarrow a^5D_{3,4}$ could be observed and show similar results. In our recent work,[7] we found that the population of the *J* components decreases from the energetically lowest state ($z^5P^o_3$) to that of the energetically highest state ($z^5P^o_1$). This could be ascribed to the relaxation process during the ejection of the excited Cr* atom from the droplet. In agreement with this observation, an evaluation of the observed emission intensities in the present work on the basis of known free atom transition probabilities[13] yields very similar level populations as in ref 7 (Table 1). To obtain the relative populations (rel. pop.) of the observed excited states, we fit the dispersed LIF lines in Figure 4 with Gaussian functions. The obtained areas and full widths at half-maxima (fwhm) are listed in Table 1. The relative populations are then calculated as the ratios of measured areas to known relative intensities (the results are normalized for each multiplet). Analogously, the averaged relative population from the PI experiments[7] is normalized. Summation of the observed intensities within each multiplet reveals that the total population numbers for $z^5P°$ and $z^7P°$ are approximately equal. The $y^7P° \rightarrow a^7S_3$ emission exceeds the other two transition pathways by more than an order of magnitude. A determination of exact ratios did not seem to be very reliable.

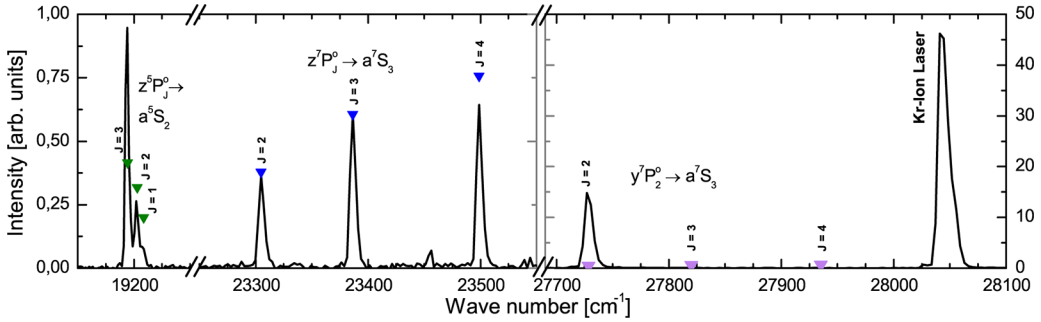

Figure 4. Spectrally resolved fluorescence of Cr atoms excited at 28056.6 cm^{-1} into the $y^7P°$ state inside He_N. The bare Cr atom transitions $z^7P^o_{2,3,4} \rightarrow a^7S_3$, $y^7P^o_{2,3,4} \rightarrow a^7S_3$, and $z^5P^o_{1,2,3} \rightarrow a^5S_2$ are indicated by triangles.[12] Note the different intensity scales on the left and right panels. The feature at 23456 cm^{-1} is an artifact due to a faulty CCD response.

dx.doi.org/10.1021/jp312336m | J. Phys. Chem. A 2013, 117, 9621−9625

Table 1. Peak Areas and Widths of the Observed Septet and Quintet Transitions[a]

transition	wavenumber (cm^{-1})[12]	measured area of emission line	measured fwhm (cm^{-1})	rel. intensity[13]	rel. LIF pop.	rel. PI pop.[7]	free atom lifetime (ns)[9]
$z^5P_3^\circ \rightarrow a^5S_2$	19194.34	7520 (190)	3.7(1)	11000	0.64(2)	0.81(18)	16.2
$z^5P_2^\circ \rightarrow a^5S_2$	19203.12	2070 (70)	3.4*	8400	0.23(2)	0.15(3)	16.2
$z^5P_1^\circ \rightarrow a^5S_2$	19208.77	710 (40)	3.4*	5300	0.13(2)	0.04(4)	16.0
$z^7P_2^\circ \rightarrow a^7S_3$	23305.01	4810 (150)	6.3(2)	10000	0.35(2)		32.2
$z^7P_3^\circ \rightarrow a^7S_3$	23386.35	7800 (170)	6.1(2)	16000	0.35(2)		31.5
$z^7P_4^\circ \rightarrow a^7S_3$	23498.84	8130 (220)	6.1(2)	20000	0.30(2)		30.3
$y^7P_2^\circ \rightarrow a^7S_3$	27728.87	274300 (3300)	8.3(2)	13000	1.00		6.6
$y^7P_3^\circ \rightarrow a^7S_3$	27820.23	0		17000	0.00		6.6
$y^7P_4^\circ \rightarrow a^7S_3$	27935.26	0		19000	0.00		6.6

[a](*) marked values were manually set in the fitting routine. Data from the literature[13] are applied for obtaining the relative population of states that is compared to PI results.[7] Uncertainties from fitting routines are given in parentheses.

The electronic relaxation from y^7P° to $z^7P^\circ_{2,3,4}$ involves a change from a $3d^44s4p$ configuration to $3d^54p$, similar to that in the relaxation to $z^5P^\circ_{1,2,3}$. Both correspond to forbidden transitions in the free atom becoming allowed due to the surrounding He. Calculations of the Cr−He potential curves could give a deeper insight into the mechanisms which are responsible for the observed relaxations.

For all three branches of emission, a linear increase of fluorescence intensity with laser power up to 9.5 W/cm^2 could be observed. In principle, this is not surprising, because the width of the excitation band is very large, giving rise to an increased saturation intensity.

To explore the time dependence of the relaxation and ejection processes, we monitored the time dependent decay of $y^7P^\circ_2 \rightarrow a^7S_3$ (27736.78 cm^{-1}), $z^7P^\circ \rightarrow a^7S_3$ (~23400 cm^{-1}), and $z^5P^\circ \rightarrow a^5S_2$ (~19200 cm^{-1}) fluorescence after the 20 ns pulse excitation of the $y^7P^\circ \leftarrow a^7S_3$ Cr-in-He_N band. Figure 5

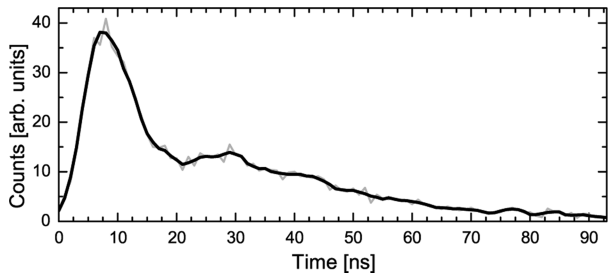

Figure 5. $z^5P^\circ \rightarrow a^5S_2$ fluorescence decay after a $y^7P^\circ \leftarrow a^7S_3$ excitation at 28090 cm^{-1}.

shows the quintet channel decay with a detection limited time resolution of 5 ns. First fluorescence emission is observed shortly after the laser pulse with a time delay barely outside our time resolution. As the low-pass filter reduced the stray light of the 28090 cm^{-1} excitation laser to the noise level of the detector system, the displayed signal resembles the time dependence of this fluorescence channel. A similar structure with two maxima followed by two different tails is observed on the $z^7P^\circ \rightarrow a^7S_3$ channels. The $y^7P^\circ \rightarrow a^7S_3$ fluorescence detection is more strongly biased by the strong laser excitation pulse due to the immediate neighborhood in wavenumber, which does not allow an unambiguous conclusion.

In the following we will summarize the observations and draw conclusions with regard to the relaxation processes.

A. Laser Excitation of the $y^7P^\circ \leftarrow a^7S_3$ Transition of Cr Attached to He_N. The absorption spectra have a width of about 400 cm^{-1} and are blue shifted by about 300 cm^{-1} compared to the free atom transitions, an observation that is in line with the previous conclusion that Cr is located inside the droplets.[7] After laser excitation, several fluorescence channels are observed with emission linewidths below the monochromator resolution (4−8 cm^{-1}), indicating that all emission takes place after ejection of Cr from the droplet. The *"most direct" channel* is represented by the $y^7P^\circ_2 \rightarrow a^7S_3$ fluorescence, irrespective of the excitation wavenumber within the 400 cm^{-1} bandwidth: Fast relaxation into the lowest *J*-level inside the droplet seems to be followed by ejection from the droplet. This pathway is chosen by the majority of the excited atoms. A *second channel* involves a normally spin-forbidden transition into $z^5P^\circ_{1,2,3}$ and ejection which we had also observed in our PI experiments.[7] In this process which is followed by a few percent of the atoms, the *J*-level population of $z^5P^\circ_{1,2,3}$ is observed with a ratio similar to that in ref 7. Time resolved measurements (Figure 5) show a first emission peak shortly after the laser pulse. A second, weaker emission maximum follows about 20 ns after the first emission peak with a decay time of 23 ± 5 ns. The *third channel* is taken by another few percent of the excited atoms with relaxation into the $z^7P^\circ_{2,3,4}$ states followed by ejection and free atom fluorescence. All three *J*-levels appear about equally populated. Time resolved measurements reveal similar emission characteristics as observed for the quintet state channel. The delayed emission peak with respect to the first fluorescence maximum must be due to a combination of different processes. If Cr atoms inside droplets, excited to higher *J*-levels (i.e., $J = 3, 4$) of $y^7P^\circ_J$, remain longer in the droplet while relaxing through lower *J* of y^7P° into z^7P° or z^5P° than those that were originally excited into $y^7P^\circ_2$, such timing of the emission could evolve.

B. Laser Excitation of the $z^7P^\circ \leftarrow a^7S_3$ Transition of Cr Attached to He_N. The large width of the excitation spectrum and its blue shift compared to the free atom transition is again in agreement with an in-droplet location of the atom, whereas the narrow fluorescence emission exclusively from the lowest *J*-level of z^7P° shows that the excited atoms quickly relax into the lowest spin−orbit state followed by ejection from the droplet. No other emission channels than $z^7P^\circ_2 \rightarrow a^7S_3$ are observed which is no surprise because all states that are lower in energy than z^7P° are metastable and would not radiatively decay as free atoms. As the emission after $z^7P^\circ \leftarrow a^7S_3$ excitation was rather weak, we were not able to perform time dependent measurements.

In summary, the excitation of a transition metal atom with rather complex electronic structure in a cold helium environ-

dx.doi.org/10.1021/jp312336m | J. Phys. Chem. A 2013, 117, 9621−9625

ment, is followed by fast relaxation processes involving both spin−orbit interaction and electronic state mixing. Detailed time-resolved measurements of all decay channels after subnanosecond excitation and detection (i.e., shorter PMT transition time) may allow us to collect the data that is necessary to develop a rate equation model for the relaxation of excited Cr in helium droplets.

AUTHOR INFORMATION

Corresponding Author

*E-mail: M.K., markus.koch@tugraz.at; W.E.E., wolfgang.ernst@tugraz.at.

Notes

The authors declare no competing financial interest.

ACKNOWLEDGMENTS

We thank Friedrich Lindebner and Matthias Hasewend for experimental assistance. This work was supported by the Austrian Science Fund (FWF, Grant 22962-N20), as well as the European Commission and the Styrian Government within the ERDF program.

REFERENCES

(1) Kromer, M.; Sim, S. A.; Fink, M.; Röpke, F. K.; Seitenzahl, I. R.; Hillebrandt, W. Double-Detonation Sub-Chandrasekhar Supernovae: Synthetic Observables for Minimum Helium Shell Mass Models. *Astrophys. J.* **2010**, *719*, 1067−1082.

(2) Welty, D. E.; Simon, T.; Hobbs, L. M. Spatial and Temporal Variations in Interstellar Absorption Towards HD 72127AB. *Mon. Not. R. Astron. Soc.* **2008**, *388*, 323−334.

(3) Blackwell, D. E.; Menon, S. L. R.; Petford, A. D. Measurement of Relative Oscillator Strengths for Cr I Lines - I. Measures for Transitions from Levels a7S3(0.00eV), a5S2(0.94eV) and a5D0−4 (0.96−1.03eV). *Mon. Not. R. Astron. Soc.* **1984**, *207*, 533−546.

(4) Pellin, M. J.; Gruen, D. M.; Fisher, T.; Foosnaes, T. Emission, Optical-Optical Double Resonance, and Excited State Absorption Spectroscopy of Matrix Isolated Chromium and Molybdenum Atoms. *J. Chem. Phys.* **1983**, *79*, 5871−5886.

(5) Callegari, C.; Ernst, W. E. Helium Droplets as Nanocryostats for Molecular Spectroscopy - from the Vacuum Ultraviolet to the Microwave Regime. In *Handbook of High-Resolution Spectroscopy*; Merkt, F.; Quack, M., Eds.; John Wiley & Sons: Chichester, U.K., 2011; Vol. 3.

(6) Ratschek, M.; Koch, M.; Ernst, W. E. Doping Helium Nanodroplets with High Temperature Metals: Formation of Chromium Clusters. *J. Chem. Phys.* **2012**, *136*, 104201−1−104201−6.

(7) Kautsch, A.; Hasewend, M.; Koch, M.; Ernst, W. E. Fano Resonances in Chromium Photoionization Spectra After Photo-induced Ejection from a Superfluid Helium Nanodroplet. *Phys. Rev. A* **2012**, *86*, 033428−1−033428−4.

(8) Koch, M.; Lanzersdorfer, J.; Callegari, C.; Muenter, J. S.; Ernst, W. E. Molecular Beam Magnetic Resonance in Doped Helium Nanodroplets. A Setup for Optically Detected ESR/NMR in the Presence of Unresolved Zeeman Splittings. *J. Phys. Chem. A* **2009**, *113*, 13347−13356.

(9) Cooper, J.; Gibson, N.; Lawler, J. Radiative Lifetimes in Cr I by Laser Induced Fluorescence. *J. Quant. Spectrosc. Radiat. Transfer* **1997**, *58*, 85−92.

(10) Loginov, E.; Drabbels, M. Excited State Dynamics of Ag Atoms in Helium Nanodroplets. *J. Phys. Chem. A* **2007**, *111*, 7504−7515.

(11) Moroshkin, P.; Hofer, A.; Weis, A. Atomic and Molecular Defects in Solid 4He. *Phys. Rep.* **2008**, *469*, 1−57.

(12) Sugar, J.; Corliss, C. Atomic-Energy Levels of the Iron-Period Elements: Potassium Through Nickel. *J. Phys. Chem. Ref. Data, Suppl.* **1985**, *14*, 1−664.

(13) Kramida, A.; Ralchenko, Y.; Reader, J. NIST ASD Team. *NIST Atomic Spectra Database* (version 5.0); National Institute of Standards and Technology, Gaithersburg, MD, 2012; http://physics.nist.gov/asd.